

Theory of Neutron Scattering in High- T_c Cuprates: Two Component Spin-Fermion Model

Yunkyu Bang

*Department of Physics, Chonnam National University, Kwangju 500-757,
and Asia Pacific Center for Theoretical Physics, Pohang 790-784, Korea*

(Dated: April 20, 2022)

Recent neutron scattering experiments have revealed that the generic form of the magnetic excitations in the high- T_c cuprates of wide range of doping has the so-called "hourglass" shape; it features both upward and downward excitations at the incommensurate (IC) momenta spanning from the resonance peak at the commensurate momentum (π, π) . We propose the two-component spin-fermion model as a minimal phenomenological model which has both local spins and itinerant fermions as independent degrees of freedom. Our calculations of the dynamic spin correlation function provide good agreement with experiments and show: (1) the upward dispersion branch of magnetic excitations is mostly due to the local spin excitations; (2) the downward dispersion branch is from collective spin excitations of fermions; (3) the resonance mode is a mixture of both degrees of freedom.

PACS numbers: 74.20.74.20-z, 74.50

The study of spin dynamics has been a key research interest since the discovery of the high- T_c superconductor because it is expected that the spin correlation holds crucial information for the mechanism of the high- T_c superconductivity (HTSC). For long the two main observations in the neutron scattering experiments of high- T_c cuprates are (1) the incommensurate (IC) peaks at low energy or at quasielastic excitations^{1,2} and (2) the so-called resonance peak at commensurate wave vector at relatively high energy ($30 \sim 50$ meV)³. In early experiments the IC peaks were observed only in the deeply underdoped lanthanum cuprate (LCO) and the resonance mode was the hallmark of the fully doped two layer yttrium cuprate (YBCO). However, later experiments reveal that both features appear in both cuprates, although sensitively depending on doping level. And with more recent experiments^{4,5,6,7,8,9}, a unifying form of the magnetic excitations in the cuprate superconductors has emerged as "hourglass" shape of excitations around the wave vector $(1/2, 1/2)$ (hereafter in units of $2\pi/a$), in which the low energy IC excitations form the downward dispersion branch and the high energy IC excitations form the upward dispersion branch, and the two branches of excitations merge at the commensurate momentum and at the resonance frequency.

It is a pressing question to understand the origin of this "hourglass" shape excitations. Theoretical proposals up to now can be classified into two groups: (1) theories based on the spin dynamics in the presence of stripes^{10,11}, and (2) Fermi liquid type theories of itinerant fermions^{12,13}. The key idea of the first group of theories is that the stripes formed by doping in the two dimensional Cu-O plane can split the commensurate spin wave excitations into two IC branches at the wave vectors $(1/2 + \epsilon, 1/2)$ and $(1/2 - \epsilon, 1/2)$ or at their symmetry rotated vector positions by $x \longleftrightarrow y$ depending on the directions of the stripes. The dispersions from each branch of the two IC modulation cross at the commensurate wave vector $(1/2, 1/2)$ at a higher energy, which can be identified as the resonance mode. This picture provides a qualitative explanation to the hourglass dispersion and the resonance mode. However, this type of theories has difficulty to be extended to the higher doping regime where the presence and the nature of

the stripes is questionable. The second group of proposals are itinerant fermion theories with interaction^{12,13}. In this type of theories, the resonance mode and the downward dispersion can be obtained, but the upward dispersion branch is not yet satisfactorily reproduced.

In this paper, we propose a two component spin-fermion model¹⁴ as a minimal phenomenological model to provide a natural and unifying explanation for the above mentioned neutron experiments of high- T_c cuprates. In this phenomenological model, the minimal set of low energy degrees of freedom are the spin wave excitations of local spins and the continuum particle-hole excitations of fermions. A similar phenomenological theory is also known as one component spin-fermion model and has been intensively studied by Pines and coworkers.¹⁵ The key difference from the one component model, is the presence of the spin wave excitations directly from the local spins in addition to the usual collective spin density excitations from fermions. Despite a gross similarity to the one component model, we argue that the necessity of the local spins for the minimal model of HTSC is impelling from the neutron experiments. In a mixed momentum and real-space representation the corresponding Hamiltonian is written as

$$H = \sum_{\mathbf{k}, \alpha} c_{\alpha}^{\dagger}(\mathbf{k}) \epsilon(\mathbf{k}) c_{\alpha}(\mathbf{k}) + \sum_{\mathbf{r}, \alpha, \beta} g \vec{\mathbf{S}}(\mathbf{r}) \cdot c_{\alpha}^{\dagger}(\mathbf{r}) \vec{\sigma}_{\alpha\beta} c_{\beta}(\mathbf{r}) + H_S, \quad (1)$$

where the first term is the fermionic kinetic energy and the second term describes the coupling between local spins $\vec{\mathbf{S}}(\mathbf{r})$ and the spin density of the conduction electrons. The last term represents an effective low-energy Hamiltonian for the local spins. When the local spins have a short range AFM correlation, the bare (before coupling to the fermions) spin correlation function has the general form as follows¹⁶.

$$\chi_{0,S}^{-1}(\mathbf{q}, \Omega) = \chi_{0,S}^{-1}(\mathbf{Q}, 0) \cdot [1 + \xi^2 |\mathbf{q} - \mathbf{Q}|^2 - \Omega^2 / \Delta_{SG}^2], \quad (2)$$

where \mathbf{Q} the 2D AFM ordering vector, and the spin gap energy Δ_{SG} and the magnetic correlation length ξ combine to give the spin wave velocity $v_s = \Delta_{SG} \cdot \xi$. Counting the coupling term

to one loop order, the dressed spin correlation functions of the model are written as follows.

$$\chi_S^{-1}(\mathbf{q}, \Omega) = \chi_{0,S}^{-1}(\mathbf{q}, \Omega) - g^2 \cdot \chi_{0,f}(\mathbf{q}, \Omega) \quad (3)$$

$$\chi_f^{-1}(\mathbf{q}, \Omega) = \chi_{0,f}^{-1}(\mathbf{q}, \Omega) - g^2 \cdot \chi_{0,S}(\mathbf{q}, \Omega) \quad (4)$$

where $\chi_{0,f}$ is the noninteracting spin susceptibility of the conduction band of the fermions and $\chi_{0,S}$ is introduced in Eq.(2).

Having two degrees of freedom in the model, two spin susceptibilities χ_S and χ_f should be calculated on equal footing. Previous studies of the local spin correlation embedded in the fermion bath¹⁶ considered only the imaginary part of $\chi_{0,f}$ (Landau damping) to damp the spin wave excitations in Eq.(3) and the real part of $\chi_{0,f}$ is assumed either already included in the local spin dynamics described in Eq.(2) or its effect unimportant. In fact, when the coupling g is weak, this approach is reasonable. But in the strong coupling limit (when the dimensionless coupling constant $\lambda \equiv g^2 \cdot \chi_{0,f}(\mathbf{Q}, 0) \cdot \chi_{0,S}(\mathbf{Q}, 0) \sim O(1)$), including both the real and imaginary parts as in the above equations is crucial. In the strong coupling limit, both spin susceptibilities $\chi_S(\mathbf{q}, \Omega)$ and $\chi_f(\mathbf{q}, \Omega)$ become a mixture of both the local spins and the itinerant fermions and they assimilate to each other with increasing the coupling strength λ .

To make a contact with experiments, we use a tight binding model for the fermion dispersion

$$\varepsilon(\mathbf{k}) = -2t(\cos(k_x) + \cos(k_y)) - 2t' \cos(k_x) \cdot \cos(k_y) - \mu. \quad (5)$$

For calculations in this paper, we chose $t' = -0.4t$, and $\mu = -0.81t$. The energy scale t and the choice of parameters t' , μ will be discussed later with the numerical results. The fermion susceptibility $\chi_{0,f}$ is calculated both in normal state (NS) and in superconducting state (SS) assuming a canonical d-wave pairing $\Delta(\mathbf{k}) = \Delta_0[\cos(k_x) - \cos(k_y)]$.

Fig.1(a) shows $Im\chi_f(\mathbf{q}, \Omega)$ scanned along $\mathbf{q} = (h, 1/2)$ in the superconducting state. The superconducting gap $\Delta_0 = 0.2t$ and the bare spin gap $\Delta_{SG} = 1.1t$ is chosen; the physical spin gap is strongly renormalized by coupling with fermions. The dimensionless coupling constant $\lambda = 0.80$ is chosen. The main effect of the coupling is to pull down the bare spin gap Δ_{SG} below the particle-hole excitation gap of $\chi_{0,f}(\mathbf{q}, \Omega)$ ($\sim 2\Delta_0$), which then forms a sharp resonance peak at $\mathbf{Q} = (1/2, 1/2)$. Centering from this resonance mode, both the downward dispersion branch and the upward dispersion branch span out. The origin of the upward dispersion is apparently from the local spin wave mode (see Eq.(2)) and the origin of the downward dispersion is the itinerant spin excitations of $\chi_{0,f}$. This fact is identified in Fig.1(b) which shows $Im\chi_{0,f}(\mathbf{q}, \Omega)$ scanned along $\mathbf{q} = (h, 1/2)$ in the superconducting state. The shape and strength of the downward whisker like excitations in $Im\chi_{0,f}$ is quite sensitive to the band structure (controlled by t, t' , etc), Fermi surface curvature (controlled by μ, t'), and the size of the d-wave gap $\Delta(\mathbf{k})$.

With the coupling strength $\lambda = 0.8$, the dressed susceptibility $\chi_f(\mathbf{q}, \Omega)$ obtains features of both the local spin susceptibility $\chi_{0,S}$ and the itinerant spin susceptibility $\chi_{0,f}$, and the

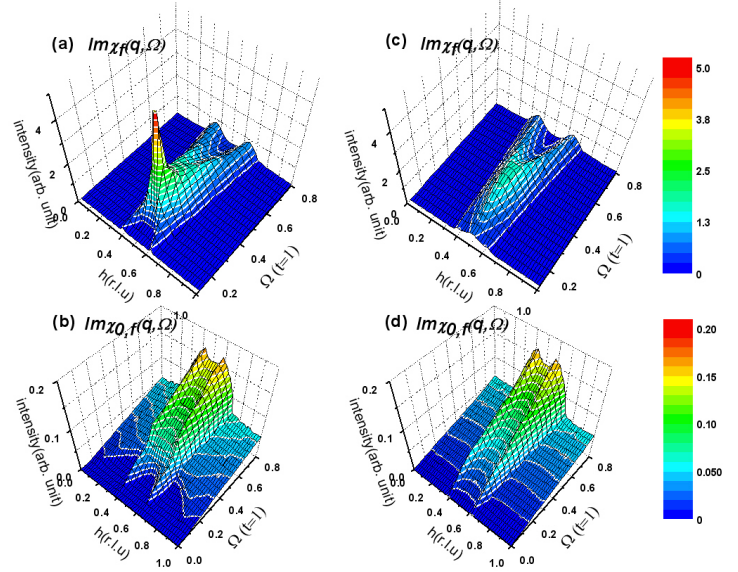


FIG. 1: (a) The dressed spin susceptibility $Im\chi_f(\mathbf{q} = (h, 1/2), \Omega)$ in superconducting state. Parameters are $\Delta_{SG} = 1.1t$, $\Delta_0 = 0.2t$, and $\lambda = 0.8$ (b) The bare spin susceptibility $Im\chi_{0,f}(\mathbf{q}, \Omega)$ in superconducting state. (c) $Im\chi_f(\mathbf{q}, \Omega)$ in normal state ($\Delta_0 = 0$). (d) $Im\chi_{0,f}(\mathbf{q}, \Omega)$ in normal state.

behavior of the dressed susceptibility $\chi_S(\mathbf{q}, \Omega)$ is qualitatively similar to the one of $\chi_f(\mathbf{q}, \Omega)$ in this coupling strength. Therefore we show only the results of $\chi_f(\mathbf{q}, \Omega)$ in Fig.1.; the experimental data of neutron scattering should be the contributions from both susceptibilities. With a smaller coupling strength ($\lambda < 0.5$) the two spin susceptibilities retain more of their original characteristics of the local spin wave and the itinerant fermion susceptibility, respectively.

Fig.1(c,d) are the same plots as in Fig.1(a,b) but in normal state. First, the resonance peak becomes a completely overdamped mode having only a hump like structure in $Im\chi_f(\mathbf{q}, \Omega)$. Second, the downward whisker like dispersion disappears because the free fermion susceptibility $\chi_{0,f}(\mathbf{q}, \Omega)$ in normal state has no such structure as seen in Fig.1(d). Lastly, the upward dispersion remains almost similar to the case of the superconducting state. In experiments the upward dispersion in normal state appears more smeared⁹. This could be due to the effect of enhanced damping process at higher temperatures which is not included in our calculations. The results of Fig.1(a,c) successfully reproduce the main features of recent neutron scattering experiments in high- T_C cuprates^{4,5,6,7,8,9}, ie., the resonance mode in superconducting state, the hourglass shape of the upward and downward dispersions, and their drastic change in normal and superconducting states. In particular, these results are in excellent agreement with the data of YBCO_{6,6}⁹.

The mechanism of forming the resonance mode in our model is illustrated in Fig.2. When the inverse of the dressed susceptibilities of Eq.(3) and Eq.(4) crosses zero (which occurs simultaneously in both susceptibilities), the dressed susceptibilities develop a resonance mode, a bound state, or a

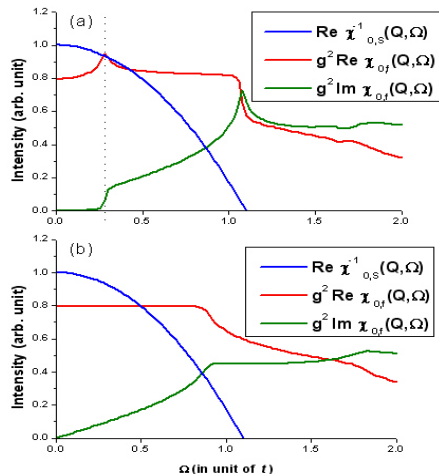


FIG. 2: (a) Plots of bare susceptibilities $\text{Re}\chi_{0,s}^{-1}(\mathbf{Q}, \Omega)$, $g^2 \text{Re}\chi_{0,f}(\mathbf{Q}, \Omega)$, and $g^2 \text{Im}\chi_{0,f}(\mathbf{Q}, \Omega)$, respectively in superconducting state. Parameters are $\Delta_{SG} = 1.1t$, $\Delta_0 = 0.2t$, and $\lambda = 0.8$. The vertical dashed line is a guide to the eyes indicating the position of pole at $\Omega = 0.28t$. (b) The same as (a) in normal state (ie. $\Delta_0 = 0$).

completely overdamped mode depending on the presence and the strength of the imaginary part at the position of pole. In Fig.2 we plot separately $\text{Re}\chi_{0,s}^{-1}(\mathbf{Q}, \Omega)$, $\text{Re}\chi_{0,f}(\mathbf{Q}, \Omega)$, and $\text{Im}\chi_{0,f}(\mathbf{Q}, \Omega)$ to make this point clear. Fig.2(a) is the case of a superconducting state. By tuning the coupling constant g and the bare spin gap value Δ_{SG} as chosen in Fig.1(a), the pole of $\chi_{f,s}(\mathbf{q} = \mathbf{Q}, \Omega)$ occurs at $\Omega_{res} \sim 0.28t$. At this frequency a small amount of $\text{Im}\chi_{0,f}$ still exists just below the p-h excitation gap, making the pole a resonance mode. Fig.2(b) shows the case of the normal state ($\Delta_0 = 0$) with the same parameters as in Fig.1(c). The position of pole occurs at a little higher frequency ($\Omega \sim 0.5t$) and there is substantial amount of damping from $\text{Im}\chi_{0,f}$ making an overdamped mode as shown in Fig.1(c). With this mechanism of damping of the pole, even in the superconducting state, a small variation of the coupling or the superconducting gap, the intensity of the resonance mode can vastly change. Finally, we would like to make a remark about the unique character of the resonance mode in our model. The line of $\text{Re}\chi_{0,s}^{-1}(\mathbf{Q}, \Omega)$ in Fig.2 is not a simple inverse of a static potential (for example, $\frac{1}{\bar{v}}$ in a RPA calculation of Hubbard model) but it carries its own dynamics and spectral density. Therefore, the resonance mode formed by coupling of two dynamic susceptibilities $\chi_{0,f}$ and $\chi_{0,s}$ should carry the spectral density from both the local spin wave and the fermion particle-hole excitations.

To make a comparison of our calculations with experiments, it is important to fix the energy scale of the model. The tight binding band of Eq.(5) is widely studied to fit the ARPES data and the estimate of t varies from 150 meV to 300 meV depending on the doping and different cuprate compounds¹⁷. Our calculation results are in good agreement with neutron

experiments in terms of energy scale if we choose $t \sim 150$ –180 meV. This value of t is somewhat low compared to the estimates from ARPES experiments. One possible reason of this discrepancy is that the extraction of t value from ARPES is carried by fitting the whole range of the quasiparticle dispersion. As a result the high energy dispersion sets the overall energy scale and the value of t . However, for calculations of the spin susceptibility the high energy quasiparticle excitations are almost irrelevant and it is the low energy quasiparticle excitations near Fermi level which determine the structure of the low energy spin susceptibility. With this reasoning it is quite possible that the effective t value near FS is in fact much smaller due to a renormalization of a strong correlation effect. Also we use the chemical potential level $\mu = -0.8t$ in our calculations. This value of μ corresponds to the band filling $n = 0.503$ in our model, which is even higher than the half filling ($n = 0.5$). In our phenomenological model the half filling has no special meaning because we do not include any strong coupling effect after the phenomenological Hamiltonian Eq.(1). On the other hand the Fermi surface (FS) curvature is the single most important parameter to control the degree of incommensurability (IC) and the strength of the downward dispersion in the free fermion susceptibility $\chi_{0,f}$ as shown in Fig.1(b). The curvature can be tuned with t' and μ in our model. We decided to fix $t' = -0.4t$ and tune the value of μ as a free parameter. Using a lower value of μ (smaller band filling), both the degree of the IC of the downward excitations and the p-h excitations gap edge have tendency to increase. Using a more realistic band with more tight binding parameters as t'' , t''' , etc., it will be possible to choose more realistic band fillings.

Fig.3.(a-d) show the constant energy scans of $\chi_f(\mathbf{q}, \Omega)$ in the superconducting state for $\Omega = 0.2t, 0.28t, 0.6t$, and $0.8t$, respectively. Constant energy scans of neutron scattering data of YBCO⁵ and LBCO⁶ show peculiar patterns of IC peak positions in (q_x, q_y) momentum space at different energy cuts. In particular, the 45 deg rotation of the patterns from a low energy scan (below the resonance energy) to a high energy scan draws special attention recently and several theoretical explanations have been proposed^{11,13}. Results of Fig.3(a-d) demonstrate that the two component spin fermion model can consistently explain this phenomena, too. First, Fig.3(c) is the scan of $\chi_f(\mathbf{q}, \Omega)$ at the resonance energy, $\Omega = 0.28t$ with the same parameters as in Fig.1(a). It shows a very intense peak at $(1/2, 1/2)$ indicating a very sharp resonance not only in energy but also in momentum space. Fig3(a) and Fig.3(b) are scans at higher energies than the resonance energy and Fig.3(d) is a scan of lower energy cut. We colored the highest intensity positions with black color to emphasize the clear patterns. The lower energy scan (Fig.3(d)) shows the IC peaks at $(1/2 \pm \delta, 1/2)$ and $(1/2, 1/2 \pm \delta)$ forming a diamond shape pattern. The higher energy scans (Fig3(a) and Fig3(b)) show that the IC peak positions at $(1/2 \pm \delta, 1/2 \pm \delta)$ and $(1/2 \pm \delta, 1/2 \mp \delta)$ forming a square shape pattern which has the symmetry of the 45 deg rotated from the low energy pattern. The results of Fig.3 excellently reproduce the observed patterns of the constant energy scan data of neutron experiments reported in YBCO⁵ and LBCO⁶.

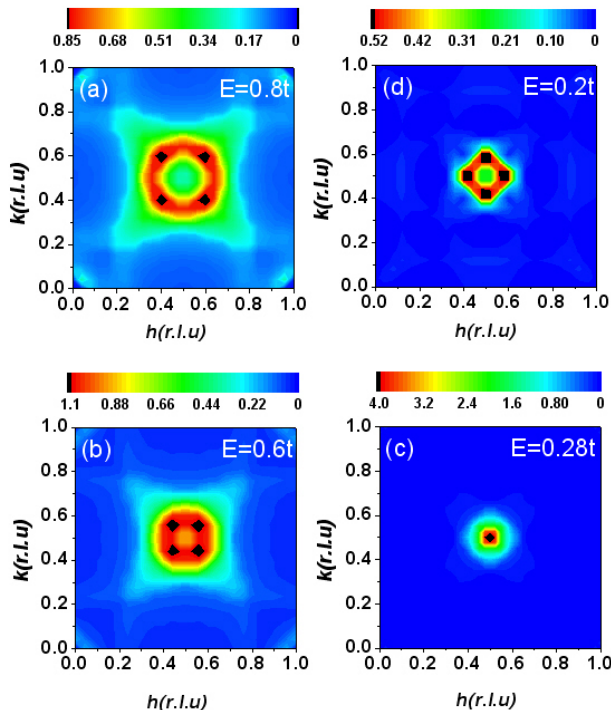


FIG. 3: Constant energy scans of $Im\chi_f(\mathbf{q}, \Omega)$ at (a) $\Omega = 0.8t$, (b) $\Omega = 0.6t$, (c) $\Omega = 0.28t$, (d) $\Omega = 0.2t$. Parameters are $\Delta_{SG} = 1.1t$, $\Delta_0 = 0.2t$, and $\lambda = 0.8$.

In our model we can trace the origins of the patterns. The low energy IC peaks and diamond shape pattern is basically a reflection of the band structure and d-wave superconducting gap. The high energy IC peaks and the square shape pattern has more complicated origin. At and above the resonance energy the dressed spin correlation χ_f is the result of a strong

interplay between the local spin correlation and the itinerant spin correlation. Therefore the high energy scan pattern is determined by a subtle interplay/competition between $\chi_{0,s}(\mathbf{q}, \Omega)$ and $\chi_{0,f}(\mathbf{q}, \Omega)$. The presence of IC peaks itself is the manifestation of the high energy spin wave dispersion spanning from the AFM wave vector \mathbf{Q} ; so the incommensurability increases with energy. However, whether the pattern becomes a square or a diamond shape has no universal mechanism. We tested various combinations of parameters t' , μ , Δ_{SG} , Δ_0 and λ . The low energy diamond shape pattern is quite robust within our model. As to the patterns of higher energy scans, although the square shape is the dominant one, it is not absolutely robust; with different parameters the diamond pattern often appears, too, at high energy scans. Therefore, we think that the 45 deg rotation of the IC peak patterns may not be a universal feature of high- T_c cuprates; it can change with doping and with different cuprate compounds.

In conclusion, we proposed a two-component spin fermion model to explain the neutron scattering experiments in high- T_c cuprates. With the two spin degrees of freedom of the local spins and the itinerant spins, our calculations of the spin correlations reproduced the essential features of the experiments: the hourglass dispersions, resonance mode, their changes in normal and superconducting states, and the IC peak patterns of the constant energy scans. With this success of the two-component spin fermion model to describe the neutron scattering experiments, the pressing question is now what the microscopic theory is for the phenomenological two-component spin fermion model; specifically how the local spin degree of freedom survives after doping from the parent insulating cuprate compounds.

We thank A. Chubukov, I. Eremin, and B. Keimer for discussions. Y. B. was supported by the KOSEF through the CSCMR and the Grant No. KRF-2005-070-C00044.

- ¹ S-W. Cheong et al., Phys. Rev. Lett. **67**, 1791 (1991).
- ² P. Dai, H. A. Mook, and F. Dogan, Phys. Rev. Lett. **80**, 1738 (1998).
- ³ H. A. Mook et al., Phys. Rev. Lett. **70**, 3490 (1993); H. Fong et al., Phys. Rev. Lett. **75**, 316 (1995); P. Dai, H. A. Mook, G. Aeppli, S. M. Hayden, and F. Dogan et al., Nature **406**, 965 (2000).
- ⁴ M. Arai et al., Phys. Rev. Lett. **83**, 608 (1999)
- ⁵ S. M. Hayden et al., Nature **429**, 531 (2004).
- ⁶ J.M. Tranquada et al., Nature **429**, 534 (2004).
- ⁷ S. Pailhes, Y. Sidis, P. Bourges, V. Hinkov, A. Ivanov, C. Ulrich, L. P. Regnault, and B. Keimer, Phys. Rev. Lett. **93**, 167001 (2004)
- ⁸ V. Hinkov et al., Nature **430**, 650 (2004).
- ⁹ V. Hinkov et al., cond-mat/0601048.
- ¹⁰ C. D. Batista, G. Ortiz, and A. V. Balatsky, Phys. Rev. B **64**, 172508 (2001);
- ¹¹ G.S. Uhrig, K.P. Schmidt, and M. Gruninger, Phys. Rev. Lett. **93**, 267003 (2004); C.D. Batista, G. Ortiz, A.V. Balatsky, cond-mat/0511303; G. Seibold and J. Lorenzana, Phys. Rev. B **73**, 144515 (2006); M. Vojta, T. Vojta, and R. K. Kaul, Phys. Rev. Lett. **97**, 097001 (2006).
- ¹² D. K. Morr and D. Pines, Phys. Rev. Lett. **81**, 1086 (1998).
- ¹³ M. R. Norman, Phys. Rev. B **75**, 184514 (2007); I. Eremin, Dirk K. Morr, A. V. Chubukov, and K. Bennemann, Phys. Rev. B **75**, 184534 (2007); I. Eremin, D. K. Morr, A. V. Chubukov, K. H. Bennemann, and M. R. Norman, Phys. Rev. Lett. **94**, 147001 (2005).
- ¹⁴ Y. Bang, I. Martin, and A. V. Balatsky Phys. Rev. B **66**, 224501 (2002); Y. Bang, M. J. Graf, N. J. Curro, and A. V. Balatsky, Phys. Rev. B **74**, 054514 (2006).
- ¹⁵ A.V. Chubukov, D.Pines, J. Schmalian, in The Physics of Superconductors, ed. K.H. Benneman and J. B. Ketterson, Berlin, Springer, 2003, and references therein.
- ¹⁶ S. Sachdev, A. V. Chubukov, and A. Sokol, Phys. Rev. B **51**, 14874 (1995).
- ¹⁷ R. S. Markiewicz, S. Sahrakorpi, M. Lindroos, H. Lin, and A. Bansil, Phys. Rev. B **72**, 54519 (2005); R. Coldea, et al., Phys. Rev. Lett. **86**, 5377 (2001); M. Norman, Phys. Rev. B **52**, 615 (1995).